TrxR1, Gsr, and oxidative stress determine hepatocellular carcinoma malignancy

Michael R. McLoughlin[a,1], David J. Orlicky[b,1], Justin R. Prigge[a,1], Pushya Krishna[a], Emily A. Talago[a], Ian R. Cavigli[a], Sofi Eriksson[a,c], Colin G. Miller[a,d], Jean A. Kundert[e], Volkan I. Sayin[f,g], Rachel A. Sabol[a,h], Joshua Heinemann[d], Luke O. Brandenberger[a], Sonya V. Iverson[a], Brian Bothner[d], Thales Papagiannakopoulos[f,i], Colin T. Shearn[j], Elias S. J. Arnér[c], and Edward E. Schmidt[a,k,2]

[a]Department of Microbiology and Immunology, Montana State University, Bozeman, MT 59718; [b]Department of Pathology, School of Medicine, University of Colorado Anschutz Medical Campus, Aurora, CO 80045; [c]Division of Biochemistry, Department of Medical Biochemistry and Biophysics, Karolinska Institute, 171 77 Stockholm, Sweden; [d]Department of Chemistry and Biochemistry, Montana State University, Bozeman, MT 59718; [e]Animal Resources Center, Montana State University, Bozeman, MT 59718; [f]Department of Pathology, New York University School of Medicine, New York, NY 10016; [g]Department of Clinical and Molecular Medicine, University of Göteborg, 405 30 Göteborg, Sweden; [h]Tulane School of Medicine, Tulane University, New Orleans, LA 70112; [i]Perlmutter Cancer Center, New York University School of Medicine, New York, NY 10016; [j]Anschutz Medical Campus, University of Colorado Denver, Aurora, CO 80045; and [k]McLaughlin Research Institute, Great Falls, MT 59405

Edited by Michael Karin, University of California San Diego School of Medicine, La Jolla, CA, and approved April 17, 2019 (received for review February 23, 2019)

Thioredoxin reductase-1 (TrxR1)-, glutathione reductase (Gsr)-, and Nrf2 transcription factor-driven antioxidant systems form an integrated network that combats potentially carcinogenic oxidative damage yet also protects cancer cells from oxidative death. Here we show that although unchallenged wild-type (WT), TrxR1-null, or Gsr-null mouse livers exhibited similarly low DNA damage indices, these were 100-fold higher in unchallenged TrxR1/Gsr–double-null livers. Notwithstanding, spontaneous cancer rates remained surprisingly low in TrxR1/Gsr-null livers. All genotypes, including TrxR1/Gsr-null, were susceptible to *N*-diethylnitrosamine (DEN)-induced liver cancer, indicating that loss of these antioxidant systems did not prevent cancer cell survival. Interestingly, however, following DEN treatment, TrxR1-null livers developed threefold fewer tumors compared with WT livers. Disruption of TrxR1 in a marked subset of DEN-initiated cancer cells had no effect on their subsequent contributions to tumors, suggesting that TrxR1-disruption does not affect cancer progression under normal care, but does decrease the frequency of DEN-induced cancer initiation. Consistent with this idea, TrxR1-null livers showed altered basal and DEN-exposed metabolomic profiles compared with WT livers. To examine how oxidative stress influenced cancer progression, we compared DEN-induced cancer malignancy under chronically low oxidative stress (TrxR1-null, standard care) vs. elevated oxidative stress (TrxR1/Gsr-null livers, standard care or phenobarbital-exposed TrxR1-null livers). In both cases, elevated oxidative stress was correlated with significantly increased malignancy. Finally, although TrxR1-null and TrxR1/Gsr-null livers showed strong Nrf2 activity in noncancerous hepatocytes, there was no correlation between malignancy and Nrf2 expression within tumors across genotypes. We conclude that TrxR1, Gsr, Nrf2, and oxidative stress are major determinants of liver cancer but in a complex, context-dependent manner.

thioredoxin reductase | glutathione reductase | Nrf2 | oxidative stress | hepatocellular carcinoma

Liver cancer is the third most lethal cancer worldwide. There is a major need to better understand the mechanisms underlying progression of the disease and to identify novel molecular targets for therapy (1). Oxidative stress in hepatocytes has been implicated in liver cancer, but the mechanisms and overall impacts remain uncertain (2, 3). Reactive oxygen species (ROS), such as hydrogen peroxide (H_2O_2), which arise primarily from respiration, metabolism, or inflammation, can cause point mutations or larger genomic lesions (4).

Since mutation underlies carcinogenesis, oxidative stress is considered carcinogenic (5–8); however, H_2O_2 is now also recognized as a signaling molecule that modulates inflammation, proliferation, differentiation, cytoprotection, autophagy, metastasis, and metabolic pathways (9–11). The activities of these pathways can either increase or decrease malignancy in a context-dependent fashion (12). Therefore, H_2O_2 likely can be either procarcinogenic or anticarcinogenic depending on context.

Excess cytosolic ROS is eliminated by peroxiredoxins using reducing power from thioredoxin reductase-1 (TrxR1) or by glutathione peroxidases using reducing power from glutathione reductase (Gsr) (11). In response to oxidative stress, nuclear factor erythroid-derived 2-like 2 (Nrf2), which is normally post-translationally repressed by Kelch-like ECH-associated protein-1 (Keap1), becomes derepressed and drives expression of components within the TrxR1- and Gsr-driven systems above their basal levels (13). Other Nrf2 target genes encode detoxification,

Significance

Oxidative DNA damage is considered carcinogenic, yet the increased oxidative stress in cancer cells could make these cells critically dependent on endogenous antioxidant systems for survival. Accordingly, activation of the major cellular antioxidant network correlates with increased malignancy in many cancers. This report shows that genetic co-disruption of the two major reductase systems within this network in mouse liver increases oxidative stress yet is apparently neither carcinogenic nor tumoricidal. Instead, chronic lifetime oxidative stress in the liver strongly augments the malignant progression of chemically induced cancers. Thus, the balance between oxidative stress and the endogenous antioxidant network is shown to have a much greater impact on determining malignant progression of cancers than on determining rates of cancer initiation.

Author contributions: E.S.J.A. and E.E.S. designed research; M.R.M., D.J.O., J.R.P., P.K., E.A.T., I.R.C., S.E., C.G.M., J.A.K., V.I.S., R.A.S., J.H., L.O.B., S.V.I., T.P., C.T.S., and E.E.S. performed research; C.T.S. and J.R.P. contributed new reagents/analytic tools; B.B., T.P., C.T.S., E.S.J.A., and E.E.S. analyzed data; and E.S.J.A. and E.E.S. wrote the paper.

The authors declare no conflict of interest.

This article is a PNAS Direct Submission.

Data deposition: The data reported in this paper have been deposited in the Gene Expression Omnibus (GEO) database, https://www.ncbi.nlm.nih.gov/geo (accession nos. GSE124444, GSE124445, and GSE124446).

[1]M.R.M., D.J.O., and J.R.P. contributed equally to this work.

[2]To whom correspondence should be addressed. Email: eschmidt@montana.edu.

This article contains supporting information online at www.pnas.org/lookup/suppl/doi:10.1073/pnas.1903244116/-/DCSupplemental.

Published online May 16, 2019.

energy metabolism, or other cytoprotective functions (14, 15). Homozygous single disruption of TrxR1, Gsr, or Nrf2 in mouse livers is benign (16–18), yet each of these conditions influences hepatic responses to oxidative stress (18–20). TrxR1 disruption activates Nrf2 (16), and mounting evidence suggests that TrxR1 is a critical participant in the redox signaling mechanism that makes Nrf2 H_2O_2-responsive (21). Together, the TrxR1-, Gsr-, and Nrf2-driven systems constitute an integrated antioxidant network (21).

Besides safeguarding normal cells from carcinogenesis, the Nrf2 pathway protects cancer cells from oxidative stress, cytotoxic immune responses, radiation therapy, and chemotherapy, any of which might otherwise kill the cancer (22–26). Indeed, many aggressive cancers have an activated Nrf2 pathway (27–30). Thus, the Nrf2 pathway itself can be either procarcinogenic or anticarcinogenic, depending on the context of its activation (21, 31). Similarly, based on its roles in eliminating cytosolic H_2O_2 but also in redox signaling and Nrf2 activation, we hypothesized that TrxR1, like H_2O_2 and Nrf2, might also have context-dependent procarcinogenic or anticarcinogenic activities.

N-diethylnitrosamine (DEN) is a procarcinogen that is activated to yield an ethyl diazonium ion by hepatocyte-specific cytochrome P450s. The reactive ethyl diazonium ion alkylates diverse substrates in the hepatocytes, including DNA (32). DEN treatment of proliferative liver (juvenile or regenerating) causes a high incidence of subsequent hepatocellular carcinoma (HCC) (33–35). Like clinical HCC, the DEN-induced rodent model is initiated by arbitrary mutations in the host's own cells. This provides carcinogenic diversity, and it models cancer progression in an isogeneic immune-competent host. Male mice are more susceptible than females to DEN-induced HCC; the sex-specific roles of signaling, cell adhesion, metabolism, and inflammation are still being resolved (34, 36–39). Glutathionylation and glucuronidation, both of which are induced by hepatic Nrf2 activation, participate in DEN detoxification (32, 40, 41).

Here we investigated the formation of either spontaneous or DEN-induced cancers in WT vs. TrxR1-, Gsr-, and TrxR1/Gsr-null livers, to characterize the impacts of the antioxidant systems on tumor initiation or progression. Although TrxR1/Gsr–double-null livers showed high levels of basal DNA damage, this was associated with a surprisingly low incidence of spontaneous liver cancer. However, our results also show that reductase-deficient livers remained susceptible to DEN-induced carcinogenesis, and that in the postinitiation phase, TrxR1 and Gsr deterred oxidative stress-driven malignant progression.

Results

TrxR1/Gsr-Null Livers Have Chronically Elevated DNA Damage Markers Yet Rarely Develop Spontaneous Cancer. Although neither TrxR1- nor Gsr-null livers show oxidative stress, mice with double-null (TrxR1/Gsr-null) livers, while still able to sustain long-term homeostasis via a backup system that uses the catabolism of methionine (Met) to support essential GSH-dependent activities (42), accumulate extensive oxidative damage (42, 43). TrxR1/Gsr-null livers also exhibit hepatomegaly, ploidy anomalies, hyperproliferation, hepatocyte death, and inflammation (42, 43). To investigate whether chronic oxidative stress in TrxR1/Gsr-null livers causes DNA damage, we immunostained liver sections for the modified histone γ-H2A.X (44). Our results show low frequencies of γ-H2A.X–positive nuclei in WT, Gsr-null, and TrxR1-null livers (~0.1–1% of hepatocytes positive), whereas ~40% of all nuclei in resting adult TrxR1/Gsr–double-null livers were γ-H2A.X–positive (Fig. 1). Since genome damage underlies cancer initiation, we expected TrxR1/Gsr-null livers to have a high rate of spontaneous cancers. However, of 32 aged mice (9–14 mo old, standard care) with TrxR1/Gsr-null livers, only 2 (6.3%) had liver tumors at harvest (Table 1). Whereas no spontaneous liver tumors were found in similar groups of mice with WT, Gsr-null, or TrxR1-null livers, in considering the high chronic level of damage in TrxR1/Gsr-null livers, their incidence of spontaneous tumors was unexpectedly low.

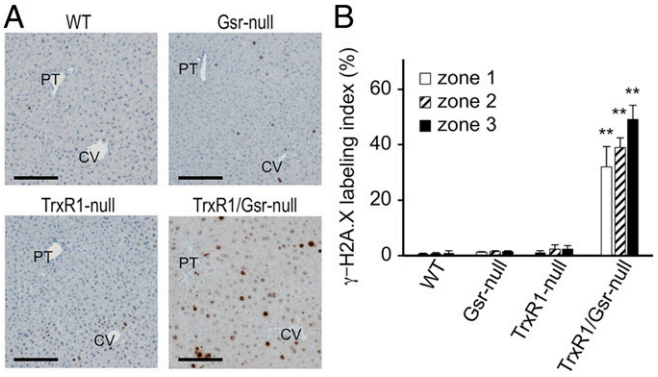

Fig. 1. TrxR1/Gsr-null livers have high basal levels of DNA damage. (*A*) Liver sections of the indicated genotypes from resting adult mice immunostained for γ-H2A.X. CV, central vein; PT, portal triad. (Scale bars: 100 μm.) (*B*) Zone- and genotype-specific staining quantification. Bars show mean and SEM. $^{**}P < 0.01$, pairwise vs. all other genotypes, Student's *t* test.

TrxR1/Gsr-Null Livers Are Susceptible to Chemically Induced Cancer. It has been hypothesized that cancer cells are more dependent on endogenous antioxidant systems compared with normal cells (45). Therefore, we tested whether the low incidence of spontaneous liver cancer in TrxR1/Gsr-null livers might reflect an intrinsic inability of liver cancer cells to thrive without these antioxidant systems, unlike noncancerous hepatocytes (42). Groups of juvenile [postnatal day (P) 14] male mice with WT, Gsr-null, TrxR1-null, or TrxR1/Gsr-null livers each received DEN, were maintained under standard care thereafter, and were harvested 8 mo later. TrxR1/Gsr-null livers readily developed severe liver cancer (Fig. 2*A*). WT and Gsr-null livers showed indistinguishable cancer burdens, TrxR1-null livers developed less cancer than WT livers, and TrxR1/Gsr-null livers developed more cancer than WT livers (Fig. 2*B*). Histology showed that the lesions in TrxR1/Gsr-null livers included large adenomas and malignant HCCs (Fig. 2*C* and *SI Appendix*, Fig. S3).

Cancer Resistance in TrxR1-Null Livers Correlates with Altered Metabolite Profiles. Following DEN challenge, mice with TrxR1-null livers developed threefold fewer tumors ($P = 0.015$) compared with their WT littermates (*SI Appendix*, Table S1). This indicates that hepatocellular TrxR1 disruption provided partial protection against DEN-induced cancer. Because TrxR1-null livers exhibit chronic activation of Nrf2 (16, 19), and the GSH system is a predominant target of Nrf2 activation, we measured basal and DEN-induced levels of Gsr and glutathione-*S*-transferase (GST) activity. Gsr activity was constitutively higher in TrxR1-null livers compared with WT livers and did not respond to the DEN challenge, whereas GST activity was constitutively higher in TrxR1-null livers compared with WT livers and was induced in both genotypes on DEN challenge (*SI Appendix*, Fig. S1 *A* and *B*). Metabolomics analyses revealed dramatic differences in metabolite profiles between WT and TrxR1-null livers in both unchallenged and DEN-challenged conditions (*SI Appendix*, Fig. S1 *C–J*). Affected metabolites included nucleosides, amino acids, and oxidative stress/repair products, and affected diverse pathways (*SI Appendix*, Fig. S1 *E–J*). This analysis verified that the basal enzymatic and metabolic profiles in mouse liver are substantially different between WT and TrxR1-null livers, and that DEN challenge differently impacts metabolic activities in each genotype.

WT and TrxR1-Null Liver Tumors Progress Similarly Under Normal Care, but TrxR1-Null Tumors Are More Aggressive Under Chronic Stress. One of the most robust ways to evaluate the impacts of mutations on

Table 1. Spontaneous tumor frequencies in mice after 9–14 mo under standard care

Genotype (*n*)	Tumors (tumors/liver)				
	Total	0.5–2 mm	2–5 mm	5–10 mm	>10 mm
WT (31)	0 (0)	0 (0)	0 (0)	0 (0)	0 (0)
Gsr-null (7)	0 (0)	0 (0)	0 (0)	0 (0)	0 (0)
TrxR1-null (22)	0 (0)	0 (0)	0 (0)	0 (0)	0 (0)
TrxR1/Gsr-null (32)	3 (0.094)	0 (0)	0 (0)	2 (0.03)	1 (0.031)

in-context cell fate is clonal analysis (46), wherein a marked subset of mutated cells develops alongside, and potentially in competition with, WT cells. To test whether persistence or progression of DEN-initiated liver cancers differs between WT and TrxR1-null cells, we used a cell lineage-tracing strategy based on clonal analysis of postinitiation marked-mosaic gene conversion (Fig. 3*A*). By this approach, the entire liver showed WT TrxR1 activity at the time of DEN exposure (P14). One month later (P44), allowing time for clonal expansion of the cancer-initiated cells, an arbitrary subset of cells was converted to TrxR1-null using limited Cre-activation (*Materials and Methods*).

At harvest, the relative contributions of functionally WT (red) and TrxR1-null (green) cells in tumors were monitored by fluorescence imaging. This analysis revealed extreme variation in the composition of TrxR1-null cells vs. WT cells to tumors (Fig. 3 *B–D*). For example, Fig. 3*B* shows a large (>1 cm diameter) tumor containing clones of red (WT) or green (TrxR1-null) cells. Fig. 3*C* shows a liver lobe containing a major tumor also composed of clones of WT or TrxR1-null cells, as well as several smaller lesions with various ratios of WT to TrxR1-null cells (quantified in Fig. 3*D*). Region 1 shows the relative representation of WT vs. TrxR1-null hepatocytes in noncancerous parenchyma of this liver. Compared with this region, cancerous regions either showed similar red:green ratios (e.g., regions 2 and 3), substantially more WT cells (regions 4 and 7), or substantially more TrxR1-null cells (regions 5 and 6). In addition, many apparently equivalent tumors were either fully WT or fully TrxR1-null (Fig. 3*E*, T1 and T2, respectively). Of 112 tumors analyzed in 25 marked mosaic animals, 55 had mixed cell composition, and 28 had predominantly WT cells, and 29 had predominantly TrxR1-null cells. Thus, even under conditions in which WT and TrxR1-null cancer cells competed with each other developmentally for contribution to tumors, neither cell type had an overarching advantage over the other within DEN-initiated liver tumors.

We next investigated whether DEN-initiated cancers in TrxR1-null vs. WT livers developed differently under conditions of lifetime chronic hepatic oxidative stress. For this, P14 male mice with WT or TrxR1-null livers were treated with 25 mg/kg DEN, and at P44, one-half of the mice were switched permanently onto drinking water containing 0.07% phenobarbital (PB) (47, 48). Metabolism of PB by hepatocyte-specific cytochrome P450s results in chronic NADPH-dependent ROS generation (49–51). At harvest (P240), most livers exhibited only few and small tumors, with the exception of TrxR1-null livers that had been under chronic PB stress, which exhibited dramatic cancer (Fig. 4*A*), including increased numbers of tumors and an increased total tumor burden (Fig. 4 *B* and *C*). Because the animals were not started on PB until 1 mo after the DEN challenge, this dramatic difference in liver cancer likely arose from differences in cancer persistence or progression rather than initiation.

Nrf2 Activity in TrxR1-, Gsr-, and TrxR1/Gsr-Null Livers. TrxR1-null livers have been shown to chronically activate Nrf2 (16, 19), whereas the status of Nrf2 activity in Gsr- and TrxR1/Gsr-null livers has not been reported. Transcriptomes of adult Gsr-null livers were similar to those of WT livers and did not have a marked Nrf2 response (*SI Appendix*, Fig. S2), whereas TrxR1/Gsr-null livers showed dramatically altered expression of hallmark Nrf2-response genes (Fig. 5*A*) (52); in the figure, red asterisks at right denote Nrf2-response genes identified in previous studies (15, 53, 54). Immunoblots confirmed that TrxR1/Gsr-null hepatocytes had increased levels of nuclear Nrf2 protein and the Nrf2-response proteins Cbr3 (carbonyl reductase-3) and HO-1 (heme-oxygenase-1) (Fig. 5*B*). TrxR1/Gsr-null livers expressed higher levels of many Nrf2-response mRNAs than have been reported for either TrxR1-null (16, 19) or Keap1-null (chronic derepression of Nrf2) livers (15) (Fig. 5*C*). Nonetheless, these comparisons also show that each genotype had a large number of responses that were either unique or were shared with only one of the other two genotypes (Fig. 5*D*), suggesting that differences in WT, TrxR1-null, TrxR1/Gsr-null, and Keap1-null liver transcriptomes extend beyond having different degrees of Nrf2 activation. qRT-PCR analyses for sentinel Nrf2-response mRNAs verified that most were not induced in Gsr-null livers yet were significantly stronger in TrxR1/Gsr-null livers compared with TrxR1-null livers (Fig. 5*E*).

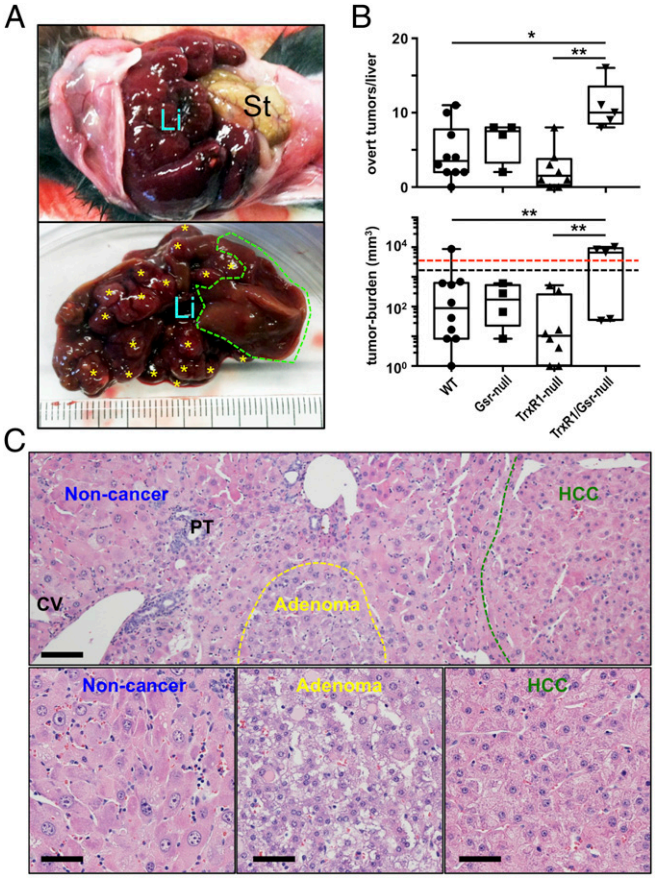

Fig. 2. DEN induces cancer in TrxR1/Gsr-null livers. Male mice were challenged with 25 mg/kg DEN at P14, maintained under standard care, and harvested at P260–P265. (*A*) Cancerous TrxR1/Gsr-null liver. The "grapeshot" appearance is from the many tumors (e.g., yellow asterisks); relatively healthy tissue is seen in the right third of the organ (green dashed line). The small ticks on the scale at the bottom are 1 mm. Li, liver; St, stomach. (*B*) Overt tumor counts (*Top*) and tumor burden (*Bottom*) of individual mice. Tumor burden represents the sum of all tumor volumes, calculated from their measured diameters. Black and red dashed lines represent the volume of normal adult WT (~1,700 mm^3) and TrxR1/Gsr-null (~3,200 mm^3) livers, respectively. $*P < 0.05$; $**P \leq 0.01$, Student's *t* test. (*C*) Representative histology of cancerous TrxR1/Gsr-null liver. (*Top*) Region containing noncancerous tissue, an adenoma, and an HCC. (*Bottom*) Higher-magnification images, as indicated. (Scale bars: *Top*, 200 μm; *Bottom*, 50 μm.)

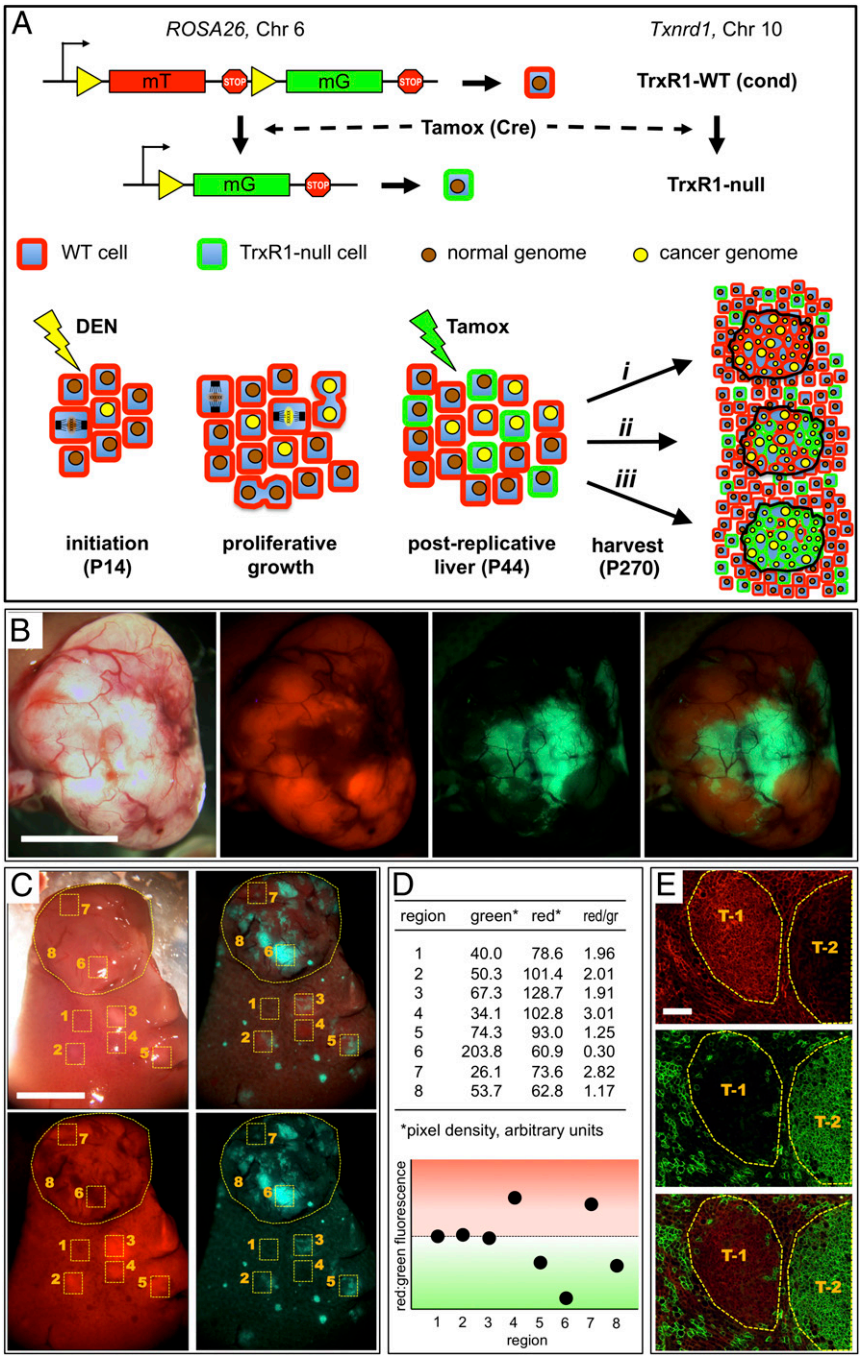

Fig. 3. Marked-mosaic analysis of cancer progression by WT vs. TrxR1-null hepatocytes. (*A*) Strategy. The dual-fluorescent Cre-responsive *ROSA*$^{mT\text{-}mG}$ allele was used to distinguish Cre-naïve (red fluorescent) from Cre-exposed (green fluorescent) cell lineages. Cre activity was supplied by activation of tamoxifen-inducible CreER. DEN (25 mg/kg) was administered i.p. to tamoxifen-naïve (functionally WT) P14 males. At P44, tamoxifen was used to induce mosaic activation of Cre in an arbitrary subset of cells. Mice were incubated under standard care and harvested at P270. If cancer cells required TrxR1, tumors were red fluorescent (condition *i*). If the absence of TrxR1 favored cancer progression, tumors were green fluorescent (*iii*). If TrxR1 was superfluous for cancer, both red and green fluorescent cells contributed (*ii*). (*B*) Contributions of WT and TrxR1 null cells within a single tumor. Bright field and red, green, and merged red + green fluorescence images are shown. (Scale bar: 1 cm.) (*C*) Diversity of WT and TrxR1-null cell contributions to tumors. Shown are bright field and red, green, and merged red + green fluorescence images of the surface of a liver lobe containing a large tumor (region 8, yellow dashed line) and several smaller lesions. (Scale bar: 1 cm.) (*D*) Relative contributions of red (WT) and green (TrxR1-null) cells were determined in the eight numbered regions circumscribed in yellow lines in *C*. Region 1 is apparently normal parenchyma; the red:green ratio in region 1 represents the baseline hepatocyte mosaicism in noncancerous liver of this animal. All other demarcated regions were cancerous. (*E*) Representative fluoromicrographs of a cryosectioned cancerous marked-mosaic liver: red (*Top*), green (*Middle*), and merged red + green (*Bottom*) fluorescence. The region exhibits two comparable tumors, one composed of WT cells (T-1, red fluorescent) and the other composed of TrxR1-null cells (T-2, green fluorescent). (Scale bar: 165 μm.)

Immunohistochemistry was used to identify the cell types that participated in the Nrf2 response in TrxR1- and TrxR1/Gsr-null livers (Fig. 6). Across genotypes, Nrf2 was largely restricted to hepatocyte nuclei. Within the liver lobule, however, the distribution was nonuniform. In WT livers, staining for Nrf2 was weak and centrilobular (zone 3, Fig. 6). Matching the transcriptome

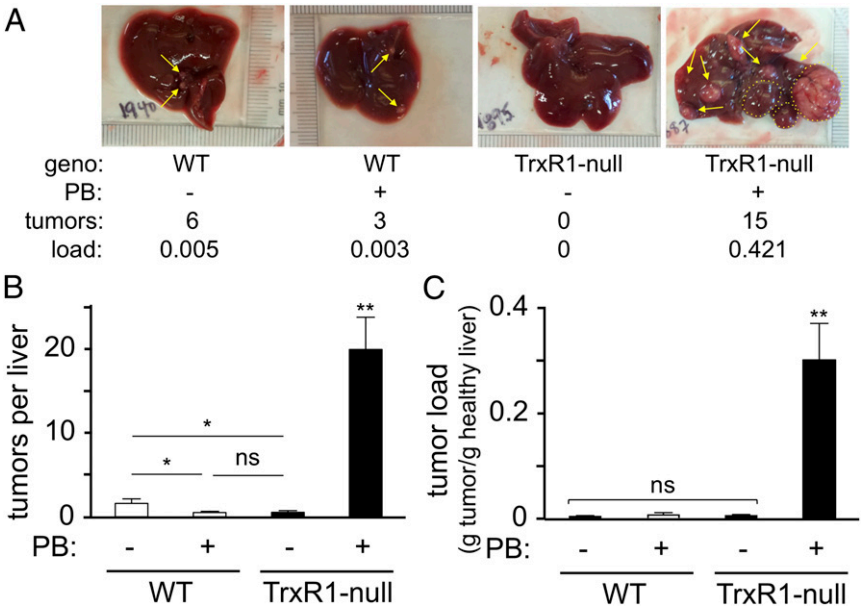

Fig. 4. Chronic post-DEN initiation PB stress promotes increased liver cancer in TrxR1-null livers. P14 male mice with constitutively WT or TrxR1-null livers were challenged with 25 mg/kg DEN. One month later, groups of mice were either maintained under standard care or switched to drinking water containing 0.07% PB. All mice were harvested at P240 ($n = 5$ mice per condition). (*A*) Gross morphology and quantification on representative whole livers of each condition at harvest. Yellow arrows and yellow dotted lines indicate visible small and large tumors, respectively. Tumor counts and loads are for the liver shown above; tumor load refers to the measured volume of tumor tissue per total liver weight for the liver shown, presented as a ratio. (*B* and *C*) Average number of tumors per liver (*B*) and tumor load (*C*) for all five animals in each condition, presented as mean and SEM. *$P < 0.05$; **$P < 0.01$; ns, $P > 0.05$, Student's *t* test.

data, proteins from Nrf2-response genes NADPH-quinone oxidase-1 (Nqo1) and Cbr3 were undetectable in WT liver (Fig. 5). Another Nrf2-response protein, HO-1, was absent from hepatocytes but was strongly expressed in Kupffer cells of WT livers (purple arrows). Since Nrf2 was not detected in Kupffer cells, this HO-1 expression was likely Nrf2-independent. In TrxR1-null livers, nuclear staining for Nrf2 protein in centrilobular hepatocytes was increased, and, correspondingly, Nqo1, Cbr3, and HO-1 were detected in centrilobular TrxR1-null hepatocytes. In TrxR1/Gsr-null livers, Nrf2 protein was enriched in nuclei across all zones, although this remained strongest in zone 3. Cbr3, Nqo1, and HO-1 were strongly increased in TrxR1/Gsr-null livers. There remained large hepatocyte-to-hepatocyte differences in expression levels of each of these proteins in TrxR1/Gsr-null livers, but the distribution was "checkerboard" rather than zonal. Nrf2 and Nrf2-response gene proteins were expressed both in apparently healthy and in degenerating hepatocytes ("ballooning" hepatocytes, blue asterisks, Fig. 6). HO-1 expression in Kupffer cells was similar in all genotypes (purple arrows), indicating that this expression was independent of the status of surrounding hepatocytes.

Phenotypic Heterogeneity in DEN-Induced Liver Tumors. DEN-induced liver tumors in each genotype were pathologically diverse, with WT, Gsr-null, TrxR1-null, and TrxR1/Gsr-null livers each exhibiting all grades of lesions, including benign hyperplasias, adenomas, and malignant HCCs (Fig. 7 and *SI Appendix*, Table S1). Quantitatively however, TrxR1/Gsr-null livers contained predominantly larger and more advanced lesions, whereas Gsr-null littermates had more benign lesions (*SI Appendix*, Fig. S3). This prompted us to ask whether there was a correlation between Nrf2 activation and tumor grade, particularly since noncancerous TrxR1- and TrxR1/Gsr-null livers showed high basal Nrf2 activity compared with WT and Gsr-null livers (Figs. 5 and 6). Sections of cancerous livers of each genotype were stained for Cbr3 and Nqo1, and protein levels were compared between normal parenchyma and cancerous lesions in the livers (Fig. 7). Within tumors of all genotypes, expression of Cbr3 and Nqo1 varied from no detectable expression in some tumors to uniformly strong expression in others (Fig. 7).

Discussion

ROS and Cytosolic Disulfide Reductase Systems in Liver Carcinogenesis. The ability of ROS to damage DNA makes these likely carcinogens. Endogenous ROS arise as collateral products of respiration, β-oxidation of fatty acids, and other activities in hepatocytes. Extracellular ROS can also impact hepatocytes. Many liver cancers are associated with inflammation (55) and are likely modulated by oxidative stress (2, 3). The cytosolic NADPH-dependent disulfide reductase systems, driven by TrxR1 and Gsr, support potent peroxidases and repair activities. Therefore, these pathways are expected to provide a critical barrier against liver carcinogenesis.

Neither TrxR1- nor Gsr-null livers show evidence of basal oxidative stress (16, 17, 20), indicating that the TrxR1- and Gsr-driven pathways robustly complement each other to combat ROS. However, TrxR1/Gsr–double-null livers accumulate extensive chronic oxidative damage. This indicates that Met-fueled reductase activity (42) by itself is insufficient to prevent pervasive oxidative stress. Contrary to our initial expectations, we found that the number of spontaneous cancers in TrxR1/Gsr-null livers remained low, yet DEN exposure increased their cancer frequency by 115-fold over the rate for unmitigated endogenous oxidants (cf. Table 1 and Fig. 2*B*). Mutation sites are likely arbitrary for both ROS and DEN. Although we are unable to quantitatively compare the one-time lesion incidence from single-dose DEN-exposure with lifetime lesion incidence from chronic oxidative stress in TrxR1/Gsr-null livers, our data might suggest that compared with alkylation damage, oxidative DNA damage is dramatically less carcinogenic. Interestingly, living organisms have been adapting to endogenous ROS since the evolution of respiration (56). In contrast, exposure to chemicals that would be metabolized into intracellular alkylating agents, as DEN is, might instead have been largely restricted to occasional environmental exposures and thus perhaps have had less impact

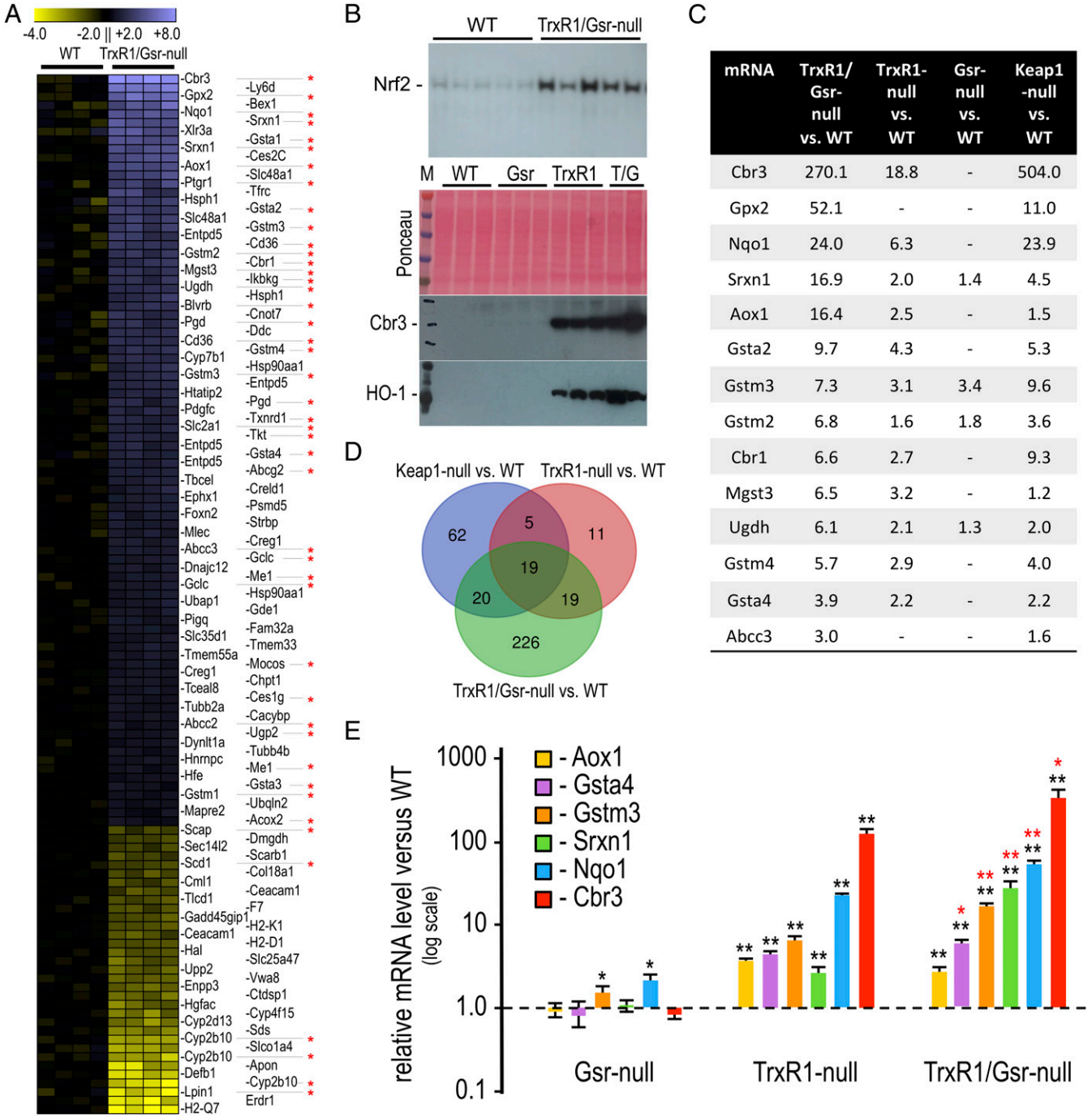

mRNA	TrxR1/Gsr-null vs. WT	TrxR1-null vs. WT	Gsr-null vs. WT	Keap1-null vs. WT
Cbr3	270.1	18.8	-	504.0
Gpx2	52.1	-	-	11.0
Nqo1	24.0	6.3	-	23.9
Srxn1	16.9	2.0	1.4	4.5
Aox1	16.4	2.5	-	1.5
Gsta2	9.7	4.3	-	5.3
Gstm3	7.3	3.1	3.4	9.6
Gstm2	6.8	1.6	1.8	3.6
Cbr1	6.6	2.7	-	9.3
Mgst3	6.5	3.2	-	1.2
Ugdh	6.1	2.1	1.3	2.0
Gstm4	5.7	2.9	-	4.0
Gsta4	3.9	2.2	-	2.2
Abcc3	3.0	-	-	1.6

Fig. 5. The Nrf2 response predominates in the transcriptome of TrxR1/Gsr-null livers compared with WT livers. (*A*) Comparative heat map of resting adult WT and TrxR1/Gsr-null liver transcriptomes. Mean values for each gene in WT livers were assigned the heat designation of black ("normal"). Red asterisks at right indicate reported Nrf2 targets. (*B*) Nrf2 protein levels in purified liver nuclei from WT and TrxR1/Gsr-null livers (*Top*) and of Cbr3 or HO-1 protein from total lysates of WT, Gsr-null, TrxR1-null, and TrxR1/Gsr-null (T/G) livers (Bottom). (*C*) Relative expression of 14 Nrf2 target genes compared with WT liver controls in TrxR1/Gsr-null (this study), TrxR1-null (16, 19), Gsr-null (this study), and Keap1-null (65) livers, analyzed using uniform criteria. (*D*) Gene list comparisons for Keap1-, TrxR1-, and TrxR1/Gsr-null livers from the uniform datasets used in *C*. (*E*) Relative mRNA levels assessed by qRT-PCR for six Nrf2 target genes in Gsr-, TrxR1-, and TrxR1/Gsr-null livers compared with basal levels in WT livers (log scale). Bars show mean and SEM; $n = 5$ for all genotypes. Black asterisks indicate values that differed significantly from WT; red asterisks represent values that differed significantly from TrxR1-null liver. $^{*}P < 0.05$; $^{**}P < 0.01$, Student's *t* test.

as a driver of natural selection over evolutionary time. If lesions induced by oxidative stress are indeed less carcinogenic than lesions induced by DEN, this would suggest that postmutation defenses (i.e., repair, tumor suppression, and immune responses) are more effective against oxidative damage than alkylation damage. Further investigations are needed to test this.

The significantly diminished tumor incidence under normal care seen in DEN-treated animals with TrxR1-null livers compared with those with WT livers (Table 1) is intriguing. Based on the strong chronic Nrf2 response (16, 19) and the altered basal- and DEN-responsive metabolome in TrxR1-null livers (*SI Appendix*, Fig. S1), it is likely that Nrf2-driven expression of the

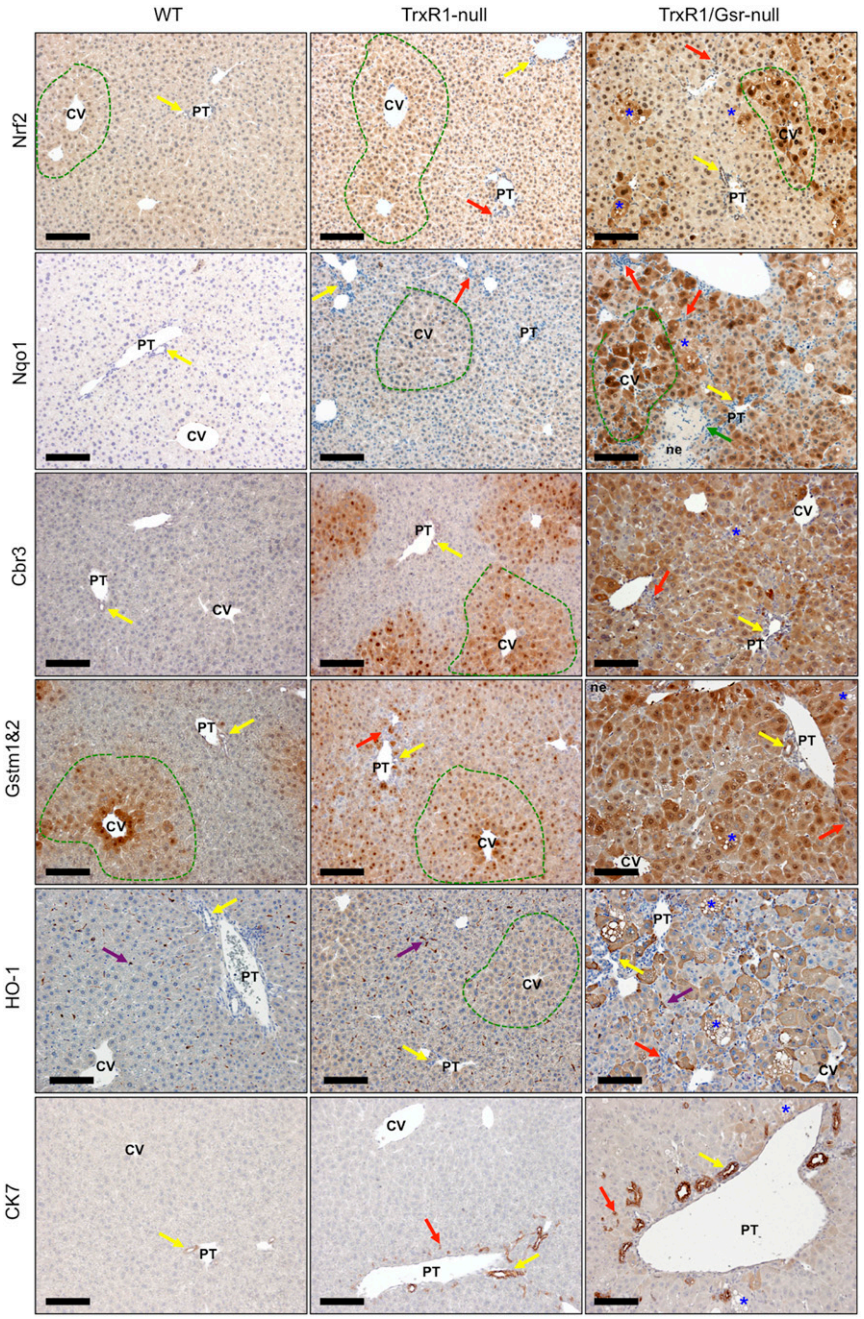

Fig. 6. Nrf2 activity in WT, TrxR1-null, and TrxR1/Gsr-null livers. Sections of livers were immunostained for the markers indicated at left (brownish-red) and counterstained with hematoxylin (bluish nuclei). Representative centrilobular (zone 3) expression circumscribed by green dashed lines. ne, necrosis. Yellow arrows, bile ducts; red arrows, ectopic ductular responses; green arrow, inflammatory cells; purple arrows, HO-1^{+} Kupffer cells. Blue asterisks denote representative ballooning (degenerating) hepatocytes. (Scale bars: 100 μm.)

phase-2 and -3 xenobiotic metabolism pathways, including both the glucuronyl and GSH conjugation systems that detoxify DEN and its products (32, 40, 41), effectively diminished the alkylation damage in these livers at the time of DEN treatment. Interestingly, the TrxR1/Gsr-null livers, in which Nrf2 target genes are induced to yet-higher levels (Fig. 5), developed more severe cancer under standard care. Although it is tempting to speculate that this reflects the balance between enhanced detoxification and increased oxidative stress, other possibilities should also be considered. For example, TrxR1-null livers overaccumulate glycogen, providing the hexose source for glucuronidation, and have an increased ability to generate excess GSH for GSH conjugation. In combination, this makes them exceptionally resistant to acetaminophen-induced hepatotoxicity (19). In contrast, TrxR1/Gsr-null livers have low glycogen levels and are critically dependent on their GSH for survival, and thus are exceptionally susceptible to acetaminophen (43). As such, the Nrf2-induced phase 2 enzymes in TrxR1/Gsr-null livers might also plausibly be substrate-limited for detoxification of DEN.

Cytosolic Disulfide Reductase Systems in Liver Cancer Persistence or Progression. Many cancers appear to be critically addicted to cytosolic disulfide reductase system activities. Metabolic realignments in cancer cells increase intracellular levels of endogenous

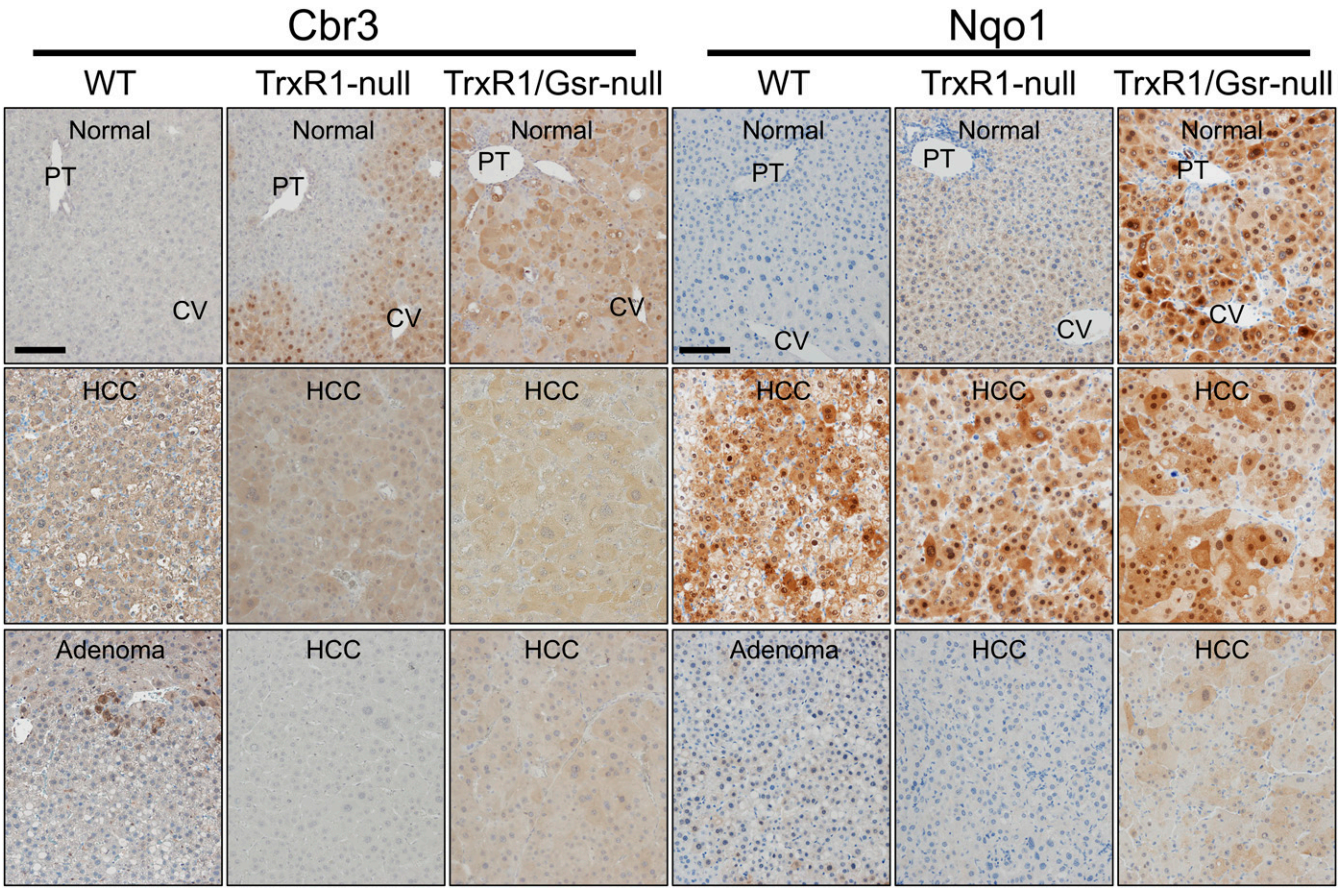

Fig. 7. Nrf2 activity in tumors. Sections of DEN-induced cancerous livers stained for expression of Cbr3 or Nqo1. The top panels represent noncancerous regions; below are representative tumors. (Scale bars: 100 μm.)

ROS and thus make the cells more susceptible to oxidative stress-induced cell death compared with noncancerous cells (45, 57). This is consistent with our own studies on inhibition of TrxR1 in cultured cancer cells, head and neck cancers, and breast cancer tumors (58), and also with a recent report showing that knockdown of TrxR1 in mouse models of xenografted human HCCs and transgene-driven mouse HCCs led to diminished tumor size (59).

In line with this, we expected HCCs to be critically dependent on the endogenous antioxidant systems, and when the oxidative damage in TrxR1/Gsr-null livers did not result in abundant fulminant HCC, we originally suspected that TrxR1/Gsr-null cancers formed but became self-limiting via a "cell suicide mechanism" that prevented transformed cells from tolerating their own cancer-associated ROS. Conversely, however, the highly abundant malignant tumors that developed in DEN-exposed TrxR1/Gsr-null livers in the present study indicate that the absence of effective endogenous cytosolic antioxidant systems is not necessarily self-limiting for HCC.

It remains unclear what roles the diversity of initiating mutations in the DEN model, followed by long-term natural selection and evolution of the tumors in the absence of the disulfide reductase systems, play in their ability to tolerate increased oxidative stress. Moreover, hepatocytic metabolic eccentricities, such as their exceptionally strong Met cycle and transsulfuration pathway, will make the Met-driven reductase pathway more robust in hepatocytic cancers (60, 61). Importantly, clinical HCC, like DEN-induced HCC, presents with diverse genetic lesions that are not well represented in some preclinical models. Moreover, long-term therapeutic efficacy will require that the cancers do not readily evolve a therapy-resistant physiology. The present study emphasizes that HCC can readily adapt and persist without TrxR1 and Gsr activities. In considering the strong propensity of cancers to acquire resistance mechanisms, therapeutic approaches targeting reductase pathways in cancers should likely be restricted to combinatorial regimes that discourage evolution of "hepatocyte-like" oxidative stress-insensitivity survival strategies.

The results presented in this study show that postinitiation oxidative stress, as modeled either by coincidental loss of both TrxR1 and Gsr (Fig. 2) or by chronic hepatic PB-induced oxidative stress in livers only lacking TrxR1 (Fig. 4), can increase liver cancer malignancy. Indeed, malignant HCCs predominated in DEN-induced TrxR1/Gsr-null livers, whereas Gsr-null livers exhibited more benign hyperplasias (*SI Appendix*, Fig. S3). Currently we do not have a mechanistic explanation for this, but three possibilities might contribute. First, it is possible that accumulated oxidative DNA damage during cancer progression favors malignant progression through a genetic mechanism, as predicted in the "multihit" hypothesis (5, 6) and suggested in at least one mouse HCC study (62). Second, it is possible that alterations in redox signaling resulting from these disruptions favor malignant progression through an epigenetic mechanism, for example, by favoring proliferation or morphogenic transitions. Third, disruption of TrxR1 and Gsr may trigger secondary enzymatic and metabolic realignments through Nrf2 (Fig. 5 and *SI Appendix*, Fig. S1) or other systems that contribute to the altered cancer phenotypes. Further investigations are needed to test each of these possibilities. The mouse liver cancer models reported here should support such investigations.

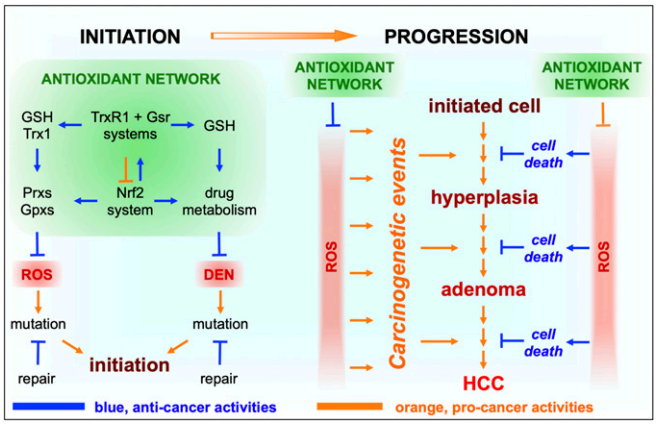

Fig. 8. Roles of the endogenous antioxidant network in cancer initiation and progression. The antioxidant systems form an integrated cross-regulated network that will effectively protect cells from carcinogens, but in existing cancers, the network likely plays both anticancer and procancer roles.

Interplay of the Cytosolic Disulfide Reductase Systems and Nrf2 in Liver Cancer. A previous study showed that in HeLa cells, pharmacologic depletion of GSH did not induce Nrf2, knockdown of TrxR1 did induce Nrf2, and combination treatments further increased Nrf2 activation (63). We now extend these observations with full liver transcriptome analyses (Fig. 5 and *SI Appendix*, Fig. S2). The distinct impacts of TrxR1-, Gsr-, and TrxR1/Gsr-null conditions on Nrf2 activation show that these three antioxidant systems are integrated into a cross-regulated network and might provide further clues to understanding Nrf2 regulation. The activities of this network optimize the protection of cells from oxidative or toxic exposures. Whereas this will effectively antagonize cancer initiation, in some cases the network could favor the malignant progression of existing tumors by preventing cell death-based defenses (Fig. 8).

A genome-wide association study of human squamous cell lung cancers revealed a strong correlation between malignancy and mutations that activate Nrf2 (29). Several mouse and human studies have also shown that malignant progression in diverse cancers is favored by chronic activation of Nrf2 (22, 27, 28), and a recent study indicated that Nrf2-deficient mice are resistant to HCC (64). Therefore, in the present study, we expected more severe liver cancers to correlate with Nrf2 activation. Conversely, we found that individual tumors within a liver can have diverse Nrf2 activity levels that show no obvious correlation with tumor grade (Fig. 7). This unexpected finding might be peculiar to liver cancers. Indeed, the diversity of molecular, genetic, redox, and metabolic phenotypes of the HCCs reported here likely presages the diversity of "programs" that individual cancers might adopt for survival. This should be considered a general caveat for studies seeking an "Achilles' heel" that makes cancer cells more susceptible than normal cells to a simple therapy.

Materials and Methods

Mice. All procedures were reviewed and approved by the Montana State University Animal Care and Use Committee. DEN was administered to male pups at P14 ± 1 d at 25 mg/kg i.p. in sterile saline (33). PB at 0.07% (wt/vol) was added to drinking water continuously starting at P44 ± 2 d. For marked-mosaic analyses, male pups at P14 ± 1 d of age, genotype *Txnrd1*$^{cond/cond}$; *ROSA*$^{mT\text{-}mG/CreER}$, were inoculated i.p. with 25 mg/kg DEN in sterile saline. At P44 ± 2 d, 0.2 mL of 1 mg/mL tamoxifen-citrate was administered i.p.

Transcriptome Analysis, qRT-PCR, Histology, and Immunohistochemistry. Transcriptomes from WT, Gsr-null, and TrxR1/Gsr-null livers were analyzed using Affymetrix 430A 2.0 arrays. Probes were synthesized from total liver RNA using the MessageAmp II-Biotin Enhanced system and hybridized for 16 h at 45 °C. Transcriptome data generated in this study have been deposited in the Gene Expression Omnibus (accession nos. GSE124444, GSE124445, and GSE124446). qRT-PCR was performed on cDNA generated from total mouse liver RNA using a mixture of oligo-dT and random primers and GoTaq PCR Master Mix. cT values were calculated using RotorGene 6000 series software v. 1.7, and differences between Nrf2-regulated transcripts compared with endogenous β-actin control were calculated. Histology, immunohistochemistry, and immunoblotting were performed following standard protocols and the antibodies listed in *SI Appendix*.

Statistical Analyses. Except where indicated in figure legends, statistical significance was determined by pairwise Student's *t* tests. Transcriptomes were analyzed using FlexArray software v. 1.6.2 and National Center for Biotechnology Information Mouse Genome Annotation 35. Array comparison output datasets were normalized by GeneChip robust multiarray averaging, and variance was calculated by one-way ANOVA. Datasets were restricted to fold change twofold or more up- or down-regulated, false discovery rate ≤0.05, and raw value expression level >200 units for comparisons between sets.

ACKNOWLEDGMENTS. We thank L. Johns, K. Shroyer, R. Molina, K. Quale, J. Graczyk, A. Holmgren, K. Williamson, M. Jerome, C. O'Rourke, M. Kavanaugh, M. Jutila, and T. Frerk for their contributions. E.E.S. was supported by the National Institutes of Health (Grants CA152559, AG040020, AG055022, and CA215784), the Wenner-Gren Foundation, the Montana Agricultural Experiment Station, and the Montana State University Department of Microbiology and Immunology. S.E. was supported by a fellowship from the Foundation Blanceflor. V.I.S. was supported by the Swedish Society for Medical Research. M.R.M. and L.O.B. were supported by scholarships from Montana State University. E.S.J.A. was supported by the Karolinska Institute, the Swedish Research Council (2013-4054 and 2014-2603), the Swedish Cancer Society (2015/238), and the Knut and Alice Wallenberg Foundation (2015/238). Infrastructure support was provided by the M. J. Murdock Charitable Trust and the National Institutes of Health (Grants GM110732 and GM103474).

1. El-Serag HB (2011) Hepatocellular carcinoma. *N Engl J Med* 365:1118–1127.
2. Marra M, et al. (2011) Molecular targets and oxidative stress biomarkers in hepatocellular carcinoma: An overview. *J Transl Med* 9:171.
3. Takaki A, Yamamoto K (2015) Control of oxidative stress in hepatocellular carcinoma: Helpful or harmful? *World J Hepatol* 7:968–979.
4. Shackelford RE, Kaufmann WK, Paules RS (2000) Oxidative stress and cell cycle checkpoint function. *Free Radic Biol Med* 28:1387–1404.
5. Nordling CO (1953) A new theory on cancer-inducing mechanism. *Br J Cancer* 7:68–72.
6. Knudson AG, Jr (1971) Mutation and cancer: Statistical study of retinoblastoma. *Proc Natl Acad Sci USA* 68:820–823.
7. Stephens PJ, et al. (2011) Massive genomic rearrangement acquired in a single catastrophic event during cancer development. *Cell* 144:27–40.
8. Ames BN, Gold LS, Willett WC (1995) The causes and prevention of cancer. *Proc Natl Acad Sci USA* 92:5258–5265.
9. Wang Z, Li Y, Sarkar FH (2010) Signaling mechanism(s) of reactive oxygen species in epithelial-mesenchymal transition reminiscent of cancer stem cells in tumor progression. *Curr Stem Cell Res Ther* 5:74–80.
10. Manda G, et al. (2015) The redox biology network in cancer pathophysiology and therapeutics. *Redox Biol* 5:347–357.
11. Sies H (2014) Role of metabolic H_2O_2 generation: Redox signaling and oxidative stress. *J Biol Chem* 289:8735–8741.
12. Singh R, Shankar BS, Sainis KB (2014) TGF-β1-ROS-ATM-CREB signaling axis in macrophage-mediated migration of human breast cancer MCF7 cells. *Cell Signal* 26:1604–1615.
13. Suzuki T, Yamamoto M (2017) Stress-sensing mechanisms and the physiological roles of the Keap1-Nrf2 system during cellular stress. *J Biol Chem* 292:16817–16824.
14. Motohashi H, Yamamoto M (2004) Nrf2-Keap1 defines a physiologically important stress response mechanism. *Trends Mol Med* 10:549–557.
15. Okawa H, et al. (2006) Hepatocyte-specific deletion of the keap1 gene activates Nrf2 and confers potent resistance against acute drug toxicity. *Biochem Biophys Res Commun* 339:79–88.
16. Suvorova ES, et al. (2009) Cytoprotective Nrf2 pathway is induced in chronically Txnrd1-deficient hepatocytes. *PLoS One* 4:e6158.
17. Rogers LK, et al. (2004) Analyses of glutathione reductase hypomorphic mice indicate a genetic knockout. *Toxicol Sci* 82:367–373.
18. Itoh K, et al. (1997) An Nrf2/small Maf heterodimer mediates the induction of phase II detoxifying enzyme genes through antioxidant response elements. *Biochem Biophys Res Commun* 236:313–322.
19. Iverson SV, et al. (2013) A Txnrd1-dependent metabolic switch alters hepatic lipogenesis, glycogen storage, and detoxification. *Free Radic Biol Med* 63:369–380.
20. Rogers LK, Bates CM, Welty SE, Smith CV (2006) Diquat induces renal proximal tubule injury in glutathione reductase-deficient mice. *Toxicol Appl Pharmacol* 217:289–298.

21. Cebula M, Schmidt EE, Arnér ES (2015) TrxR1 as a potent regulator of the Nrf2-Keap1 response system. *Antioxid Redox Signal* 23:823–853.
22. Gorrini C, et al. (2014) Estrogen controls the survival of BRCA1-deficient cells via a PI3K-NRF2-regulated pathway. *Proc Natl Acad Sci USA* 111:4472–4477.
23. Leinonen HM, Kansanen E, Pölönen P, Heinäniemi M, Levonen AL (2014) Role of the Keap1-Nrf2 pathway in cancer. *Adv Cancer Res* 122:281–320.
24. Niture SK, Jaiswal AK (2013) Nrf2-induced antiapoptotic Bcl-xL protein enhances cell survival and drug resistance. *Free Radic Biol Med* 57:119–131.
25. Zhan L, et al. (2012) Regulatory role of KEAP1 and NRF2 in PPARγ expression and chemoresistance in human non–small-cell lung carcinoma cells. *Free Radic Biol Med* 53:758–768.
26. DeNicola GM, et al. (2011) Oncogene-induced Nrf2 transcription promotes ROS detoxification and tumorigenesis. *Nature* 475:106–109.
27. Chio IIC, et al. (2016) NRF2 promotes tumor maintenance by modulating mRNA translation in pancreatic cancer. *Cell* 166:963–976.
28. Romero R, et al. (2017) Keap1 loss promotes Kras-driven lung cancer and results in dependence on glutaminolysis. *Nat Med* 23:1362–1368.
29. Cancer Genome Atlas Research Network (2012) Comprehensive genomic characterization of squamous cell lung cancers. *Nature* 489:519–525.
30. Sanchez-Vega F, et al. (2018) Oncogenic signaling pathways in the cancer genome atlas. *Cell* 173:321–337 e10.
31. Mitsuishi Y, Motohashi H, Yamamoto M (2012) The Keap1-Nrf2 system in cancers: Stress response and anabolic metabolism. *Front Oncol* 2:200.
32. Verna L, Whysner J, Williams GM (1996) N-nitrosodiethylamine mechanistic data and risk assessment: Bioactivation, DNA-adduct formation, mutagenicity, and tumor initiation. *Pharmacol Ther* 71:57–81.
33. Maeda S, Kamata H, Luo JL, Leffert H, Karin M (2005) IKKbeta couples hepatocyte death to cytokine-driven compensatory proliferation that promotes chemical hepatocarcinogenesis. *Cell* 121:977–990.
34. Tolba R, Kraus T, Liedtke C, Schwarz M, Weiskirchen R (2015) Diethylnitrosamine (DEN)-induced carcinogenic liver injury in mice. *Lab Anim* 49(Suppl 1):59–69.
35. Caviglia JM, Schwabe RF (2015) Mouse models of liver cancer. *Methods Mol Biol* 1267: 165–183.
36. Naugler WE, et al. (2007) Gender disparity in liver cancer due to sex differences in MyD88-dependent IL-6 production. *Science* 317:121–124.
37. Ma WL, Jeng LB, Lai HC, Liao PY, Chang C (2014) Androgen receptor enhances cell adhesion and decreases cell migration via modulating β1-integrin-AKT signaling in hepatocellular carcinoma cells. *Cancer Lett* 351:64–71.
38. Bigsby RM, Caperell-Grant A (2011) The role for estrogen receptor-alpha and prolactin receptor in sex-dependent DEN-induced liver tumorigenesis. *Carcinogenesis* 32: 1162–1166.
39. Wands J (2007) Hepatocellular carcinoma and sex. *N Engl J Med* 357:1974–1976.
40. Chan JY, Stout DL, Becker FF (1986) Protective role of thiols in carcinogen-induced DNA damage in rat liver. *Carcinogenesis* 7:1621–1624.
41. Teeter LD, et al. (1993) Activation of distinct multidrug-resistance (P-glycoprotein) genes during rat liver regeneration and hepatocarcinogenesis. *Mol Carcinog* 8:67–73.
42. Eriksson S, Prigge JR, Talago EA, Arnér ES, Schmidt EE (2015) Dietary methionine can sustain cytosolic redox homeostasis in the mouse liver. *Nat Commun* 6:6479.
43. Prigge JR, et al. (2017) Hepatocyte hyperproliferation upon liver-specific co-disruption of thioredoxin-1, thioredoxin reductase-1, and glutathione reductase. *Cell Rep* 19: 2771–2781.
44. Tanaka T, Halicka HD, Huang X, Traganos F, Darzynkiewicz Z (2006) Constitutive histone H2A.X phosphorylation and ATM activation, the reporters of DNA damage by endogenous oxidants. *Cell Cycle* 5:1940–1945.
45. Trachootham D, Alexandre J, Huang P (2009) Targeting cancer cells by ROS-mediated mechanisms: A radical therapeutic approach? *Nat Rev Drug Discov* 8:579–591.
46. Wieschaus E, Gehring W (1976) Clonal analysis of primordial disc cells in the early embryo of *Drosophila melanogaster*. *Dev Biol* 50:249–263.
47. Lee GH (2000) Paradoxical effects of phenobarbital on mouse hepatocarcinogenesis. *Toxicol Pathol* 28:215–225.
48. Sakurai T, Maeda S, Chang L, Karin M (2006) Loss of hepatic NF-kappa B activity enhances chemical hepatocarcinogenesis through sustained c-Jun N-terminal kinase 1 activation. *Proc Natl Acad Sci USA* 103:10544–10551.
49. Wu Q, Zhang YH, Zhao X, Shi WL, Pu XP (2011) Proteome studies on liver tissue in a phenobarbital-induced rat model. *Eur J Pharmacol* 670:333–340.
50. Shaik IH, Mehvar R (2010) Cytochrome P450 induction by phenobarbital exacerbates warm hepatic ischemia-reperfusion injury in rat livers. *Free Radic Res* 44:441–453.
51. Dostalek M, et al. (2008) Development of oxidative stress by cytochrome P450 induction in rodents is selective for barbiturates and related to loss of pyridine nucleotide-dependent protective systems. *J Biol Chem* 283:17147–17157.
52. Prigge JR, Schmidt EE (2019) Data from "Resting adult mouse Gsr-null and TrxR1/Gsr-null liver transcriptome data." National Center for Biotechnology Information–Gene Expression Omnibus. Available at https://www.ncbi.nlm.nih.gov/geo/query/acc.cgi?acc=GSE124446. Deposited December 27, 2018.
53. Wu KC, Cui JY, Klaassen CD (2011) Beneficial role of Nrf2 in regulating NADPH generation and consumption. *Toxicol Sci* 123:590–600.
54. Reisman SA, Yeager RL, Yamamoto M, Klaassen CD (2009) Increased Nrf2 activation in livers from Keap1-knockdown mice increases expression of cytoprotective genes that detoxify electrophiles more than those that detoxify reactive oxygen species. *Toxicol Sci* 108:35–47.
55. Sun B, Karin M (2013) Inflammation and liver tumorigenesis. *Front Med* 7:242–254.
56. Miller CG, Holmgren A, Arnér ESJ, Schmidt EE (2018) NADPH-dependent and -independent disulfide reductase systems. *Free Radic Biol Med* 127:248–261.
57. Harris IS, et al. (2015) Glutathione and thioredoxin antioxidant pathways synergize to drive cancer initiation and progression. *Cancer Cell* 27:211–222.
58. Stafford WC, et al. (2018) Irreversible inhibition of cytosolic thioredoxin reductase 1 as a mechanistic basis for anticancer therapy. *Sci Transl Med* 10:eaaf7444.
59. Lee D, et al. (2019) Induction of oxidative stress through inhibition of thioredoxin reductase 1 is an effective therapeutic approach for hepatocellular carcinoma. *Hepatology* 69:1768–1786.
60. Mosharov E, Cranford MR, Banerjee R (2000) The quantitatively important relationship between homocysteine metabolism and glutathione synthesis by the transsulfuration pathway and its regulation by redox changes. *Biochemistry* 39:13005–13011.
61. Stipanuk MH (2004) Sulfur amino acid metabolism: Pathways for production and removal of homocysteine and cysteine. *Annu Rev Nutr* 24:539–577.
62. Kakehashi A, et al. (2017) Progression of hepatic adenoma to carcinoma in *Ogg1* mutant mice induced by phenobarbital. *Oxid Med Cell Longev* 2017:8541064.
63. Fourquet S, Guerois R, Biard D, Toledano MB (2010) Activation of NRF2 by nitrosative agents and H_2O_2 involves KEAP1 disulfide formation. *J Biol Chem* 285:8463–8471.
64. Ngo HKC, Kim DH, Cha YN, Na HK, Surh YJ (2017) Nrf2 mutagenic activation drives hepatocarcinogenesis. *Cancer Res* 77:4797–4808.
65. Yates MS, et al. (2009) Genetic versus chemoprotective activation of Nrf2 signaling: Overlapping yet distinct gene expression profiles between Keap1 knockout and triterpenoid-treated mice. *Carcinogenesis* 30:1024–1031.